Crystalline GaSb-core optical fibers with room-temperature photoluminescence

S. SONG,[1] N. HEALY,[2] S. K. SVENDSEN,[1] U. L. ÖSTERBERG,[3] A. V. CUERVO COVIAN,[4] J. LIU,[4] A. C. PEACOCK,[5] J. BALLATO,[6] F. LAURELL,[7] M. FOKINE,[7] AND U. J. GIBSON[1,7,*]

[1]*Department of Physics and Porelabs, Norwegian University of Science and Technology, N-7491 Trondheim, Norway*
[2]*Emerging Technology and Materials Group, Newcastle University, Newcastle NE1 7RU, UK*
[3]*Department of Electronic Systems, Norwegian University of Science and Technology (NTNU), N-7491 Trondheim, Norway*
[4]*Thayer School of Engineering, Dartmouth College, Hanover, NH 03755, USA*
[5]*Optoelectronics Research Centre, University of Southampton, Southampton SO17 1BJ, UK*
[6]*Department of Materials Science and Engineering, Clemson University, Clemson, SC 29634, USA*
[7]*Department of Applied Physics, KTH Royal Institute of Technology, Stockholm 10044, Sweden*
*ursula.gibson@ntnu.no

Abstract: Glass-clad, GaSb-core fibers were drawn and subsequently laser annealed. The as-drawn fibers were found to be polycrystalline, possess Sb inclusions, and have oxide contamination concentrations of less than 3 at%. Melting and resolidifying regions in the cores using 10.6 μm CO_2 laser radiation yielded single crystalline zones with enhanced photoluminescence (PL), including the first observation of strong room temperature PL from a crystalline core fiber. Annealed fibers show low values of tensile strain and a bandgap close to that of bulk GaSb.

OCIS codes: (060.2270) Fiber characterization; (060.2390) Fiber optics, infrared; (160.6000) Semiconductor materials

---

References and links

1. J. Ballato, T. Hawkins, P. Foy, B. Yazgan-Kokuoz, C. McMillen, L. Burka, S. Morris, R. Stolen, and R. Rice, "Advancements in semiconductor core optical fiber," Opt. Fiber Technol. **16**(6), 399–408 (2010).
2. J. Ballato, T. Hawkins, P. Foy, C. McMillen, R. Stolen, and R. Rice, "Progress in crystalline semiconductor core optical fibers," in *Optical Components and Materials VII*, S. Jiang, M. J. F. Digonnet, J. W. Glesener, and J. C. Dries, eds. (SPIE, 2010), Vol. **7598**, p. UNSP 759815.
3. A. C. Peacock, J. R. Sparks, and N. Healy, "Semiconductor optical fibres: progress and opportunities," Laser Photonics Rev. **8**(1), 53–72 (2014).
4. A. C. Peacock, U. J. Gibson, and J. Ballato, "Silicon optical fibres - past, present, and future," Adv. Phys. **X**, 114–127 (2016).
5. X. Ji, S.-Y. Yu, S. Lei, H. Y. Cheng, S. Chaudhuri, W. Liu, S. Mohney, J. Badding, and V. Gopalan, "Single Crystal Small Core Semiconductor Optical Fibers for All-Fiber Optoelectronics," in *Conference on Lasers and Electro-Optics (2017), Paper SM2K.5* (Optical Society of America, 2017), p. SM2K.5.
6. N. Healy, S. Mailis, T. D. Day, P. J. Sazio, J. V. Badding, and A. C. Peacock, "Laser Annealing of Amorphous Silicon Core Optical Fibers," in *Advanced Photonics Congress (2012), Paper STu1D.1* (Optical Society of America, 2012), p. STu1D.1.
7. N. Healy, M. Fokine, Y. Franz, T. Hawkins, M. Jones, J. Ballato, A. C. Peacock, and U. J. Gibson, "CO₂ Laser-Induced Directional Recrystallization to Produce Single Crystal Silicon-Core Optical Fibers with Low Loss," Adv. Opt. Mater. **4**(7), 1004–1008 (2016).
8. E. F. Nordstrand, A. N. Dibbs, A. J. Eraker, and U. J. Gibson, "Alkaline oxide interface modifiers for silicon fiber production," Opt. Mater. Express **3**(5), 651–657 (2013).
9. F. H. Suhailin, N. Healy, Y. Franz, M. Sumetsky, J. Ballato, A. N. Dibbs, U. J. Gibson, and A. C. Peacock, "Kerr nonlinear switching in a hybrid silica-silicon microspherical resonator," Opt. Express **23**(13), 17263–17268 (2015).
10. L. Lagonigro, N. Healy, J. R. Sparks, N. F. Baril, P. J. A. Sazio, J. V. Badding, and A. C. Peacock, "Low loss silicon fibers for photonics applications," Appl. Phys. Lett. **96**(4), 041105 (2010).

11. H. Ren, O. Aktas, Y. Franz, A. F. J. Runge, T. Hawkins, J. Ballato, U. J. Gibson, and A. C. Peacock, "Tapered silicon core fibers with nano-spikes for optical coupling via spliced silica fibers," Opt. Express **25**(20), 24157–24163 (2017).

12. A. C. Peacock, J. Campling, A. F. J. Runge, H. Ren, L. Shen, O. Aktas, P. Horak, N. Healy, U. J. Gibson, and J. Ballato, "Wavelength Conversion and Supercontinuum Generation in Silicon Optical Fibers," IEEE J. Sel. Top. Quantum Electron. **24**(3), 1–9 (2018).

13. R. He, P. J. A. Sazio, A. C. Peacock, N. Healy, J. R. Sparks, M. Krishnamurthi, V. Gopalan, and J. V. Badding, "Integration of gigahertz-bandwidth semiconductor devices inside microstructured optical fibres," Nat. Photonics **6**(3), 174–179 (2012).

14. P. Mehta, N. Healy, T. D. Day, J. R. Sparks, P. J. A. Sazio, J. V. Badding, and A. C. Peacock, "All-optical modulation using two-photon absorption in silicon core optical fibers," Opt. Express **19**(20), 19078–19083 (2011).

15. R. He, T. D. Day, M. Krishnamurthi, J. R. Sparks, P. J. A. Sazio, V. Gopalan, and J. V. Badding, "Silicon p-i-n Junction Fibers," Adv. Mater. **25**(10), 1461–1467 (2013).

16. F. A. Martinsen, B. K. Smeltzer, M. Nord, T. Hawkins, J. Ballato, and U. J. Gibson, "Silicon-core glass fibres as microwire radial-junction solar cells," Sci. Rep. **4**(1), 6283 (2015).

17. A. C. Peacock and N. Healy, "Semiconductor optical fibres for infrared applications: A review," Semicond. Sci. Technol. **31**(10), 103004 (2016).

18. A. Gumennik, E. C. Levy, B. Grena, C. Hou, M. Rein, A. F. Abouraddy, J. D. Joannopoulos, and Y. Fink, "Confined in-fiber solidification and structural control of silicon and silicon-germanium microparticles," Proc. Natl. Acad. Sci. U.S.A. **114**(28), 7240–7245 (2017).

19. N. D. Orf, O. Shapira, F. Sorin, S. Danto, M. A. Baldo, J. D. Joannopoulos, and Y. Fink, "Fiber draw synthesis," Proc. Natl. Acad. Sci. U.S.A. **108**(12), 4743–4747 (2011).

20. D. A. Coucheron, M. Fokine, N. Patil, D. W. Breiby, O. T. Buset, N. Healy, A. C. Peacock, T. Hawkins, M. Jones, J. Ballato, and U. J. Gibson, "Laser recrystallization and inscription of compositional microstructures in crystalline SiGe-core fibres," Nat. Commun. **7**, 13265 (2016).

21. J. R. Sparks, R. He, N. Healy, M. Krishnamurthi, A. C. Peacock, P. J. A. Sazio, V. Gopalan, and J. V. Badding, "Zinc Selenide Optical Fibers," Adv. Mater. **23**(14), 1647–1651 (2011).

22. P. J. A. Sazio, J. R. Sparks, R. He, M. Krishnamurthi, T. C. Fitzgibbons, S. Chaudhuri, N. F. Baril, A. C. Peacock, N. Healy, V. Gopalan, and J. V. Badding, "Templated growth of II-VI semiconductor optical fiber devices and steps towards infrared fiber lasers," Solid State Lasers Xxiv Technol. Devices **9342**, 93420A (2015).

23. C. Hou, X. Jia, L. Wei, A. M. Stolyarov, O. Shapira, J. D. Joannopoulos, and Y. Fink, "Direct atomic-level observation and chemical analysis of ZnSe synthesized by in situ high-throughput reactive fiber drawing," Nano Lett. **13**(3), 975–979 (2013).

24. J. Ballato, T. Hawkins, P. Foy, C. McMillen, L. Burka, J. Reppert, R. Podila, A. M. Rao, and R. R. Rice, "Binary III-V semiconductor core optical fiber," Opt. Express **18**(5), 4972–4979 (2010).

25. B. L. Scott and G. R. Pickrell, "Fabrication of GaSb optical fibers," in *Processing and Properties of Advanced Ceramics and Composites V: Ceramic Transactions* (John Wiley & Sons, 2013), Vol. **240**, p. 65.

26. S. Song, N. Healy, U. Österberg, M. Fokine, T. Sørgård, A. Peacock, U. J. Gibson, and U. J. Gibson, "GaSb-core Optical Fibers," in *Frontiers in Optics 2017* (Optical Society of America, 2017), p. JW4A.117.

27. Y. Mizokawa, O. Komoda, and S. Miyase, "Long-time air oxidation and oxide-substrate reactions on GaSb, GaAs and GaP at room temperature studied by X-ray photoelectron spectroscopy," Thin Solid Films **156**(1), 127–143 (1988).

28. N. Healy, S. Mailis, N. M. Bulgakova, P. J. A. Sazio, T. D. Day, J. R. Sparks, H. Y. Cheng, J. V. Badding, and A. C. Peacock, "Extreme electronic bandgap modification in laser-crystallized silicon optical fibres," Nat. Mater. **13**(12), 1122–1127 (2014).

29. M. Fokine, A. Theodosiou, S. Song, T. Hawkins, J. Ballato, K. Kalli, and U. J. Gibson, "Laser structuring, stress modification and Bragg grating inscription in silicon-core glass fibers," Opt. Mater. Express **7**(5), 1589–1597 (2017).

30. R. A. Noack and W. B. Holzapfel, "Photoluminescence of GaSb under hydrostatic pressure," Solid State Commun. **28**(2), 177–179 (1978).

31. E. T. R. Chidley, S. K. Haywood, A. B. Henriques, N. J. Mason, R. J. Nicholas, and P. J. Walker, "Photoluminescence of GaSb grown by metal-organic vapour phase epitaxy," Semicond. Sci. Technol. **6**(1), 45–53 (1991).

32. M. Wu and C. Chen, "Photoluminescence of high-quality GaSb grown from Ga- and Sb-rich solutions by liquid-phase epitaxy," J. Appl. Phys. **72**(9), 4275–4280 (1992).

1. Introduction

Crystalline semiconductor cores in glass optical fibers are of great interest due to their large non-linear optical coefficients and their potential for use in devices incorporating both optical and electronic functionality. The literature on Group IV semiconductor-core glass fibers is now significant [1–5], including processing improvements [6–8] and device demonstrations [9–17]. There are also reports on both SiGe alloy and II-VI core fibers [18–23], one including

low temperature photoluminescence [21]. However, there is limited information on III-V semiconductor-core fibers [26–28] manufactured by either CVD or molten-core techniques. InSb [24] and GaSb [25] fibers have been drawn using the molten-core approach, with crystallographic and compositional properties reported. Oxidation was significant in both studies, and optical properties, other than low transmission, were not described. III-V materials are of particular interest because of their direct bandgap and potential utility as light sources, rather than as waveguides. Accordingly, further investigation of these materials is warranted, focused on emission rather than transparency.

Based on results with Group IV alloy-core fibers [7], laser annealing is a promising approach for improving the structure of III-V compound cores. GaSb, which exhibits rapid oxidation, even at room temperature [27] but should be stabilized by encapsulation in glass, is of particular interest. In this paper, we report on the structure of, and photoluminescence from, GaSb-core fibers with relatively low oxygen content, both as-drawn and after CO_2 laser annealing. Post-fabrication treatment creates single crystal regions, improves purity, and increases the photoluminescence intensity.

2. Experimental

The molten-core approach was used for the fabrication of the fibers; 99.9% pure GaSb pellets were loaded into Duran glass tubes of 7-8 mm outer diameter (o.d.) and 3-4mm inner diameter (i.d.). These preforms were torch-heated until the semiconductor melted and the glass softened. GaSb has a melting point of 712°C and a thermal expansion coefficient of 7.75×10^{-6}/K, a volume increase of ~7-8% results upon solidification. Two types of cladding glass, with softening temperatures close to the melting point of the core, were used to test the influence of the preform mechanical properties during the drawing process. The softening point of Duran is about 825 and the thermal expansion coefficient is 3.3×10^{-6}/K. Fibers also were drawn with an AR-glas cladding (5 mm o.d, 3mm i.d.), which has a softening temperature of 720°C and a thermal expansion coefficient of 9×10^{-6}/K. The AR-glas was expected to better accommodate the volume changes of the core than the Duran, both during solidification and afterwards. However, Duran proved to be a better host for annealing, as the walls of the AR-glas tubing deformed during the heating and drawing process. All fibers in this initial study were hand-drawn, with core sizes ranging from 80 to 150μm.

Annealing was performed using a 25W RF-excited CO_2 laser operated with a wavelength of 10.6μm and a pulse-width modulated supply to vary the power. This led to melting of and visible thermal emission from the core, which was observed in real time using a ThorLabs CCD camera and a 10x microscope objective. For structural studies, the CO_2 laser was scanned longitudinally along the sample for a distance of 3-4 mm at a speed of 0.01 mm/s, using a laser power between 15 and 25W. For the photoluminescence studies, localized (spot) annealing was used to make samples with annealed and as-drawn material in immediately adjacent areas. The laser power was increased slowly until the core material melted (as indicated by a change in emissivity) over a region ~300 μm in length along the fiber, then the power was reduced over 60 seconds to minimize stress in the annealed regions. The AR-glas clad fibers were not annealed.

Raman characterization was made with a Renshaw InVia system with a wavelength of 785 nm. Photoluminescence was measured using a Horiba LabRAM system with 1064 nm excitation delivered through the 50x objective used for emitted light collection.

X-ray diffraction was performed at the Diamond Light Source synchrotron, in Didcot, Oxfordshire (UK). The instrument was operated at 16.8 keV in transmission mode.

Scanning electron microscopy (SEM) and elemental studies were performed using a FEI Quanta FEG600 with Energy Dispersive X-ray spectroscopy (EDS).

3. Results and discussion

3.1 Electron microscopy

Selected samples were cleaved and polished to better image and analyze the cross-sectional structure. Figure 1 provides a SEM image of part of the core and an EDS line-scan across the core/clad interface of an as-drawn fiber. The dashed circle in Fig. 1(a) contains a feature with a slightly higher brightness in the backscattered imaging mode, indicative of a higher atomic number (Z) material. It was identified as segregated Sb, confirmed by Raman measurements (inset). The line-scan in Fig. 1(b) demonstrates that there is relatively low (~3%) oxygen inclusion in the core. Interestingly, there is a gallium deficit in the vicinity of the interface; this may be due to oxidation of the gallium, with subsequent segregation of the oxide to the interface. Formation of gallium oxides would be consistent with the observation of elemental Sb inclusions in the core and suggests that compositionally improved fibers may result either with a suitable interface modifier, or if excess Ga is added into the preform prior to molten core fiber fabrication.
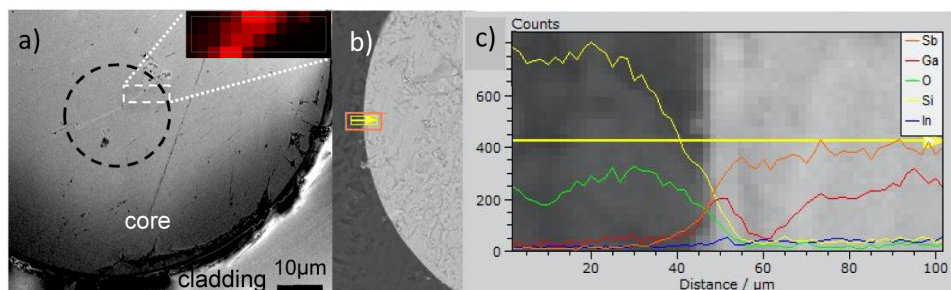

Fig. 1. a) Scanning electron micrograph of the core of a GaSb fiber. The brighter diagonal stripe within the dashed circle is elemental Sb, as shown by the intensity of the Sb Raman line at 150 cm^{-1} (inset). b) Overview of EDS linescan area; the brittle core leads to some texture. c) EDS linescan (counts) across the glass-core interface, showing segregation of Ga.
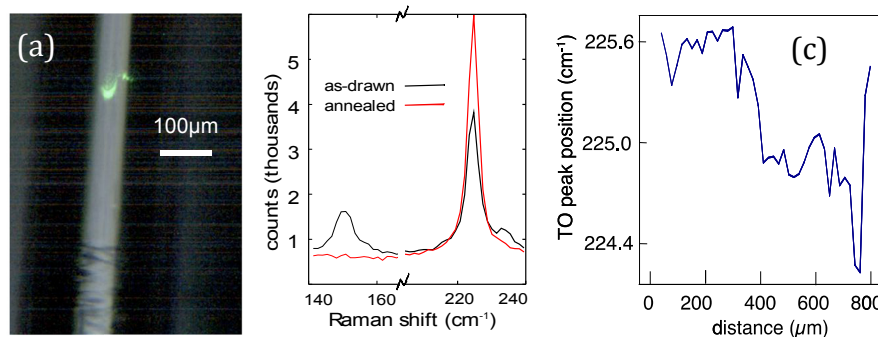
3.2 Raman spectroscopy

Fig. 2. a) Optical microscopy image of the Raman-excitation laser spot on the fiber core, showing as-drawn material with Sb striations near the image bottom, and uniform material after laser annealing, above. b) Raman spectrum of as-drawn (black) and annealed (red) regions of GaSb in Duran glass cladding. c) Raman scan from as-drawn to annealed region.

Raman results show that the GaSb material is crystalline and validate the SEM observation of excess antimony. Figure 2(a) provides a photographic image of a sample with an 80µm core, taken using the Raman microscope. The bottom ~30% of the sample shown in Fig. 2(a) was not annealed, and exhibits striations associated with the polycrystalline nature and excess Sb. The upper (as shown in the image) part of the sample was recrystallized by scanning the CO_2

laser along the fiber. Figure 2(b) provides the Raman spectrum for each of these regions. The peak at 150 cm^{-1} (as-drawn fiber) is associated with elemental Sb, while the main peak at 223 cm^{-1} is from the transverse optical (TO) mode for GaSb, and the shoulder at ~235 cm^{-1} is from the longitudinal optical (LO) mode. After annealing, the peak at 150 cm^{-1} is no longer present; the CO_2 laser has drawn excess Sb to the last-heated region, similar to the formation of Ge-rich regions in SiGe [20]. The LO mode also disappears, due to a change in the crystallographic orientation of the core. This change is observed for all annealed fibers, suggesting a strong preferential crystallographic orientation of the GaSb material in the core after laser treatment.

The GaSb TO peak position indicates different strain levels for the cladding glasses used, and after laser treatment. For a wafer or a polished pellet of the source GaSb material, and for AR-glas clad fibers sampled at 35 points, the peak position was 225.6 cm^{-1}. For Duran, the TO peak of the as-drawn material has an average shift of 225.84 cm^{-1} indicating slight compression, and a change to a tensile value of 224.98 cm^{-1} was observed for the annealed fibers. Figure 2(c) shows the peak position, scanning from the as-drawn to annealed core regions. While the strain induced shifts are significantly smaller than those observed for annealed silicon-core glass fibers [28], the data supports the observation [29] that controlled cooling rate can alter the residual strain in crystalline core fibers.

3.3 X-ray diffraction

Although Raman spectroscopy is an excellent tool for initial studies of the material structure, it is less sensitive to the degree of crystallinity, as peak widths are only slightly affected by grain size. X-ray diffraction was used to study the as-drawn and longitudinally annealed samples with the results shown in Fig. 3. Prior to annealing, Fig. 3(a) shows the core phase is polycrystalline with elemental Sb also present. After annealing, as seen in Fig. 3(b), the elemental Sb is absent, and for the GaSb, only one set of planes can be observed at any fiber rotational position. The inset shows the deviation of the azimuthal angle of the diffraction spot on the detector as the fiber is translated, with variations less than ± 0.04 degrees from the average position. A single orientation was observed for the entire 2-3 mm annealed region of the fiber suggesting that larger single crystals could be produced [7, 20] with a longer fiber. The annealed core material exhibited minimal strain and the clean, strong diffraction spot indicated that the crystal is of good quality.
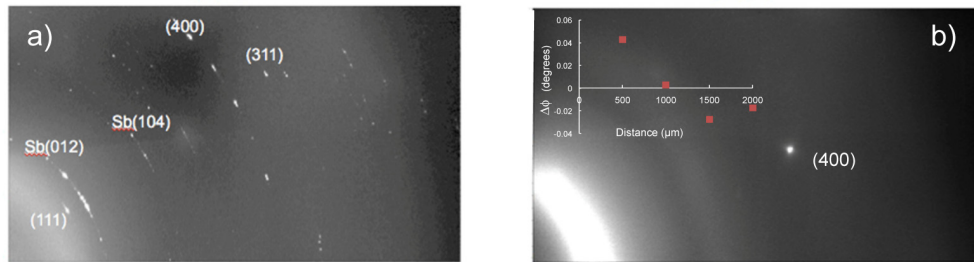

Fig. 3. X-ray diffractogram from a) as-drawn and b) annealed regions of a GaSb fiber, showing formation of single crystal GaSb. Inset shows the change in azimuthal angle ($\Delta\phi$) for a given diffraction spot when translating along the annealed fiber. Index-only labels are for GaSb.

3.4 Photoluminescence

Figure 4 shows room temperature photoluminescence (PL) spectra for as-drawn and annealed regions of Duran-clad GaSb fibers; the periodic structure is an artifact of the data acquisition program. Two Lorentzian curves were fit to each of the PL spectra to accommodate the observed asymmetry with a minimum of fitting parameters. The longer wavelength (lower energy) peak, associated with band-edge emission, shifted slightly during annealing. For the

as-drawn material, the center wavelength was at 1724 nm (0.719 eV), while the peak for the annealed material was centered at 1710 nm (0.725 eV).

The significantly increased yield and slightly higher energy emission observed for the annealed material is attributed to the improvement in crystal structure and stoichiometry of the samples with annealing, rather than stress, because the Raman spectra show only minor shifts. Stress-induced changes in the bandgap have been observed for single crystals grown by liquid phase epitaxy [30], but the stress levels in these fibers are small, and the tensile stress indicated by Raman would be expected to produce a redshift, based on both bulk and strained layer thin-film studies [31].
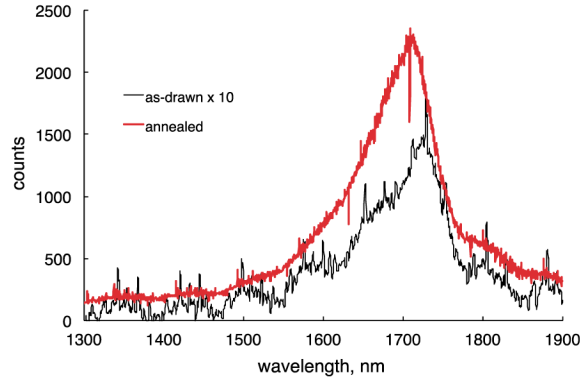

Fig. 4. Room temperature photoluminescence (PL) of as-drawn and annealed portions of the GaSb-core fiber. The as-drawn data is scaled up by a factor of 10 and has the background subtracted to ease comparison of curve shapes.

4. Conclusion

The molten-core drawing technique was used to fabricate glass-clad GaSb fibers with core diameters of 80-150 μm. As-drawn material had metallic Sb inclusions in the solidified core, due to gallium either lost to evaporation or incorporated as oxides at the interface. Laser annealing was used to draw the excess Sb away from the region of interest and to recrystallize the core. As Sb solidifies last, translation of the melt zone, or gradual cooling of the core is akin to liquid phase epitaxy of GaSb in a Sb-rich solution, and the solidifying material forms a single crystal. After annealing, the GaSb cores of annealed fibers luminesce at the wavelength predicted by a fit to temperature-dependent data on bulk samples [32], suggesting that the molten-core fiber drawing technique, with suitable post-fabrication treatment, may soon be usable for the production of infrared sources.